

# NUMERICAL SIMULATION OF HYDROGEN RELEASE FROM HIGH-PRESSURE STORAGE VESSEL

Zheng, J.Y.<sup>1\*</sup>, Bie, H.Y.<sup>1</sup>, Xu, P.<sup>2</sup>, Zhao, Y.Z.<sup>1</sup> and Liu, Y.L.<sup>1</sup>

<sup>1</sup> Institute of Process Equipment, Zhejiang University, Hangzhou, 310027, China

<sup>2</sup> Institute of Applied Mechanics, Zhejiang University, Hangzhou 310027, China

## ABSTRACT

In this paper, the deflagration region and characteristics of the hydrogen flow which was generated by high-pressure hydrogen discharge from storage vessels were studied. A 3-D analytic model is established based on the species transfer model and the SST  $k-\omega$  turbulence model. The established model is applied to the research of the flow characteristics of the hydrogen under-expanded jet under different filling pressures of 30 MPa, 35 MPa and 40 MPa, respectively. The evolution process of hydrogen combustible cloud is analyzed under the filling pressure of 30 MPa. It is revealed that a supersonic jet is formed after the high-pressure hydrogen discharge outlet. In the vicinity of the Mach disk, the hydrogen jet velocity and temperature reach the maximum values, and the variation of filling pressure has little effect on the peak values of the hydrogen jet flow velocity and temperature during the considered pressure range. In the rear of the Mach disk, the variation rates of the hydrogen flow velocity and temperature are inversely proportional to the hydrogen filling pressure. At the preliminary stage, the discharged hydrogen is apple-shaped, which expands along the radial, and then the axial growth rate of the hydrogen cloud increases with the passage of time.

## 1.0 INTRODUCTION

The environment pollution and energy shortage problems have become more and more serious around the world. Hydrogen is regarded to be one of the important energy carriers in the future because of its advantages such as high conversion efficiency, clean combustion product and low storage cost. Thus it is a good choice for the energy supply for the fuel cell vehicles (FCV). High-pressure hydrogen storage technique has become one of the most effective methods for commercialization among the existing hydrogen storage methods [1]. In order to satisfy the requirements of design and employment, the working pressure of the onboard hydrogen storage tanks is commonly higher than 30 MPa. Once the hydrogen is released from the high-pressure storage tank and comes into contact with fire, the catastrophic calamity may appear. Currently, the high-pressure hydrogen jet have attracted more and more attention of many researchers [2-5].

Due to the high fatalness of hydrogen and cost of experiments, there are few experimental studies on high-pressure hydrogen jet. And thus the numerical simulation method is a good approach. For experimental studies, Takeno et al. [6] had conducted some experimental investigation on hydrogen leakage diffusion and hydrogen detonation. Takeno et al. [6] revealed that the explosion power depends not only on the concentration and volume of hydrogen/air pre-mixture, but also on the turbulence characteristics before ignition. Shirvill et al. [7] also carried out the hydrogen diffusion experiments of pipeline jet under different pressures of 2.5 MPa and 13.5 MPa and different

apertures of 12 mm and 3 mm, in which the hydrogen concentration was calculated by testing oxygen concentration. The jet flame shape and temperature after hydrogen being ignited were also studied.

Also, some researchers have devoted to the numerical simulation of hydrogen leakage. Olvera [8] employed the standard  $k-\varepsilon$  turbulence model to simulate the effect of buildings on hydrogen diffusion, in which the results showed that the hazard of indoor hydrogen leakage was bigger than that of compressed natural gas. Wilkening and Baraldi [9] also employed numerical simulation method to investigate the danger region of hydrogen leak diffusion in pipelines. They discovered that the danger region induced by the hydrogen leakage from pipelines was smaller than that by the compressed natural gas leakage. Granovski [10] developed a 3-D diffusion model to study the hydrogen leak diffusion in atmosphere, in which the simulation results showed that the influence of buoyancy on hydrogen diffusion became smaller with increasing environment wind velocity.

The PRD (Pressure Relief Devices) installed on the high-pressure hydrogen storage vessel will open and discharge the contents when exposed to flame impingement. A hydrogen under-expanded jet is generated near the outlet of the PRD, and its characteristics are closely related to the hydrogen diffusion, the propagation of the hydrogen cloud and the detonation of the released hydrogen after ignited. In this paper, a 3-D analytic model was established to study the hydrogen jet resulting from PRD activation using the commercial CFD software FLUENT. In the proposed model, the SST  $k-\omega$  turbulence model was combined with species transfer model to study the high-pressure hydrogen release process. Besides, the flow characteristics of the high-pressure hydrogen under-expanded jet and the flammable region of the discharged hydrogen were analyzed.

## **2.0 SIMULATION MODEL AND NUMERICAL CALCULATION METHOD**

### **2.1 Calculation Model**

In the following analysis, the composite hydrogen storage vessel which is composed of Al-carbon fiber/epoxy composites is used as object to establish the analytic model. The length of the tank is 900 mm, the external diameter is 400 mm. The PRD is installed on the vessel. The size of the computational domain in the simulation is 10m (L)×10m(W)×10m(H) and an unstructured mesh with 761799 cells is adopted as shown in Fig. 1. When the pressure inside is higher than the activated pressure or the temperature is higher than the activated temperature, hydrogen can be discharged from PRD and the relief caliber is 10 mm. The initial calculation conditions are listed in Table 1.

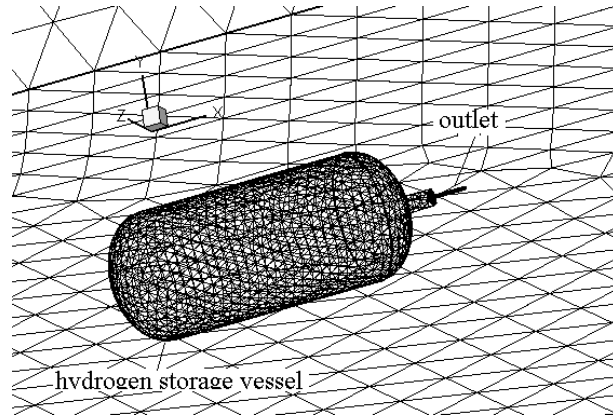


Figure 1. The CFD cells in the simulation

Table 1. Initial calculation conditions

Hydrogen filling pressure (MPa)	Hydrogen temperature (K)	Environmental temperature (K)	Environmental pressure (MPa)	Discharge coefficient
30				
35	350	300	0.1	0.85
40				

## 2.2 Turbulence Model

The release process of hydrogen discharged from the high-pressure storage vessels is confirmed as an unsteady process. In this study, the SST  $k-\omega$  turbulence model is employed to simulate the unsteady process. In the near-wall zone, the  $k-\omega$  function is adopted to calculate the fluxion in order to realize the utilization of local grid refinement. In the high Reynolds number region of principal turbulent introduce the  $k-\varepsilon$  function because the  $\omega$  given by the  $k-\omega$  function for the principal turbulent is too sensitive. A weight function is used to implement the smooth transition between the  $k-\omega$  function in the near-wall zone and the  $k-\varepsilon$  function in the principal turbulent region [11]. The turbulent viscosity function is modified considering the impact of turbulent shear stress as well as cross-diffusion term, and thus it is suitable to calculate under-expanded high-speed jet flow field formed by the high-pressure hydrogen discharge.

The turbulence kinetic energy  $k$  and the specific dissipation rate  $\omega$  can be obtained from the following transport equations:

$$\frac{\partial}{\partial t}(\rho k) + \frac{\partial}{\partial x_i}(\rho k u_i) = \frac{\partial}{\partial x_j}(\Gamma_k \frac{\partial k}{\partial x_j}) + G_k - Y_k \quad (1)$$

and

$$\frac{\partial}{\partial t}(\rho \omega) + \frac{\partial}{\partial x_i}(\rho \omega u_i) = \frac{\partial}{\partial x_j}(\Gamma_\omega \frac{\partial \omega}{\partial x_j}) + G_\omega - Y_\omega + D_\omega \quad (2)$$

where  $G_k$  - turbulence kinetic energy generated due to mean velocity gradients;  $G_\omega$  - turbulence kinetic energy generated by  $\omega$ ;  $\Gamma_k$ ,  $\Gamma_\omega$  - effective diffusivities of  $k$  and  $\omega$ , respectively;  $Y_k$ ,  $Y_\omega$  - dissipations of  $k$  and  $\omega$  due to turbulence.  $D_\omega$  represents the cross-diffusion term, which can be calculated as below:

$$D_\omega = 2(1 - F_1)\rho\sigma_{\omega,1}\frac{1}{\omega}\frac{\partial k}{\partial x_j}\frac{\partial \omega}{\partial x_j} \quad (3)$$

where  $F_1$  - blending function;  $\sigma_{\omega,1}$  - a constant,  $\sigma_{\omega,1} = 1.0$ .

The turbulent viscosity equation of SST  $k - \omega$  model is calculated as follows:

$$\mu_t = \frac{\rho k}{\omega} \frac{1}{\max\left[\frac{1}{\alpha^*}, \frac{SF_2}{\alpha_1\omega}\right]} \quad (4)$$

where  $\alpha^*$  - turbulent viscosity correlated with the flow of low-Reynolds-number;  $\alpha_1$  - a constant,  $\alpha_1 = 0.31$ ;  $S$  - strain rate magnitude.  $F_2$  is also blending function which is given by

$$F_2 = \tanh\left(\left(\max\left[2\frac{\sqrt{k}}{0.09\omega y}, \frac{500\mu}{\rho y^2\omega}\right]\right)^2\right) \quad (5)$$

where  $y$  - the distance to the next surface.

### 2.3 Species Transport Equations

Species transport model is employed to simulate the diffusion of high-pressure hydrogen release. In this model, there are two species i.e. hydrogen inside the vessel and air outside the vessel. The mass fraction  $Y_i$  of each species  $i$  can be predicted through the solution of species transport and diffusion conservation equation. The conservation equation takes the following general form:

$$\frac{\partial}{\partial t}(\rho Y_i) + \nabla \cdot (\rho \vec{v} Y_i) = -\nabla \cdot \vec{J}_i + R_i \quad (6)$$

where  $R_i$  - net rate of production of species  $i$  by chemical reaction;  $\vec{J}_i$  - diffusion flux of species  $i$ .

In turbulent flow of hydrogen release and expanding process, the mass diffusion rate is written as:

$$\vec{J}_i = -\left(\rho D_{i,m} + \frac{\mu_t}{S_{c_i}}\right) \nabla Y_i \quad (7)$$

where  $\mu_t$  - turbulent viscosity;  $S_{c_i}$  - turbulent Schmidt number;  $D_{i,m}$  - diffusion coefficient for species  $i$  in the mixture.

As large expansion ratio high-speed jet is formed due to high-pressure hydrogen discharge, the condensability of the gas should be taken into account, and the gas density is controlled by the compressible gas equation, which is expressed as:

$$\rho = P / [RT(\sum_{i=1}^m Y_i / M_i)] \quad (8)$$

where  $R$  - gas constant;  $T$  - temperature, K;  $M_i$  - molecular weight of species  $i$ .

### 3.0 SIMULATION RESULTS AND ANALYSIS

If the car is firing, the pressure and temperature inside the pressure vessel on the car will gradually increase. When they reach the corresponding activated values, the PRD will open to discharge hydrogen into the atmosphere. Since the hydrogen density is small and the ratio of pressures in and out the vessel is great, and a large expansion ratio hydrogen supersonic jet is generated. When the filling pressure is 30 MPa, the contours of predicted velocity vector and Mach number near the outfall at  $t=0.5s$  are shown in Fig. 2. Hydrogen release of large expansion ratio caused a distinct shock structure in the vicinity of outfall, the Mach disk induced was  $7D$  away from the outfall, in which  $D$  is the outfall diameter, and its diameter was about  $1.5D$ . The hydrogen's Mach number reached the maximum value just prior to the Mach disk, and the hydrogen velocity was 2,780 m/s, while a low-speed airflow vortex existed in the rear of the Mach disk.

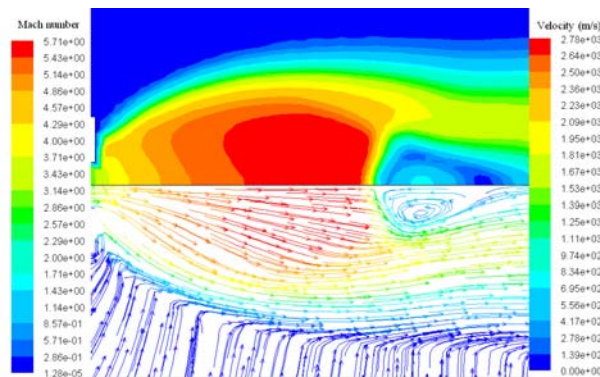


Fig. 2. Images of velocity and mach number near the outfall

Fig. 3 shows the Mach number of jet flow formed by hydrogen release from 30 MPa storage vessel at different locations. It can be seen that the Mach number gradually increases along the axial direction within  $L/D < 7$  and  $L$  is the axial distance between measuring point and outfall. The diameter of the jet flow core region is about  $2D$ . At  $L/D=7.5$ , just in the rear of mach disk, the peak values of radial Mach number transiently reduced to 1.97, and a low-speed region with a diameter  $1.04D$  was formed in the jet center. Since there was an airflow vortex in that region, the flow Mach number decreases when  $R$  increases, in which  $R$  is the distance between the measuring point and the axis. The Mach number reaches the lowest value 0.21 at  $R/D=0.52$  and then gradually increases.

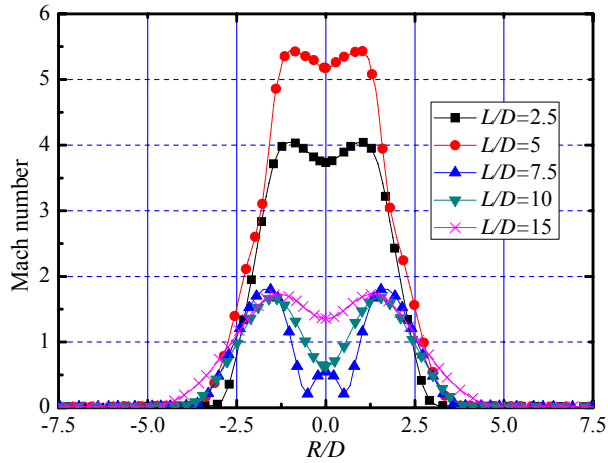
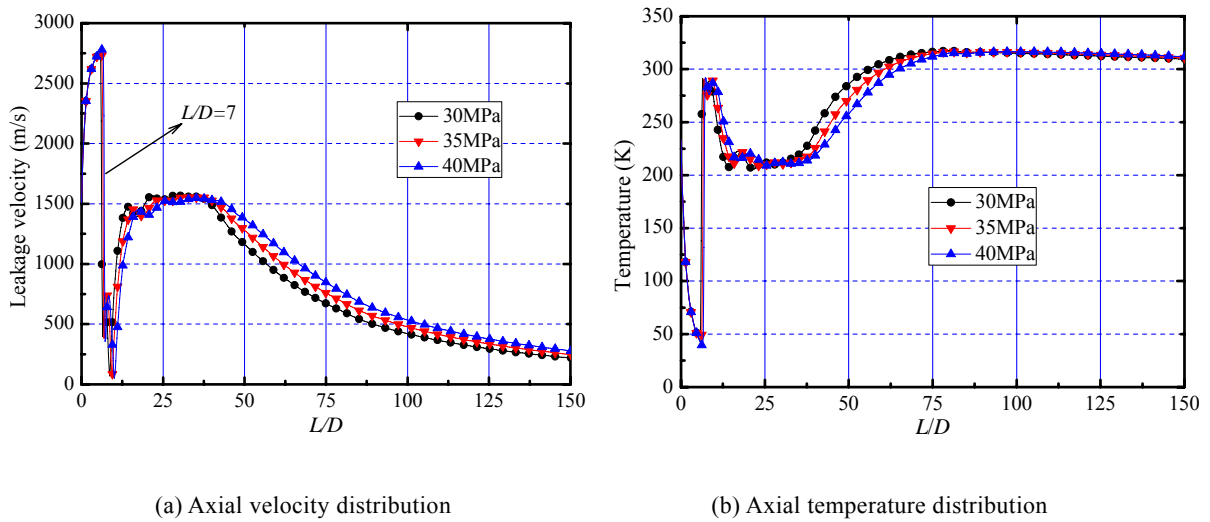


Figure 3. Mach number along radial direction at different locations

In order to study the jet flow characteristics of hydrogen leakage at different filling pressure, simulation of hydrogen release under different filling pressures of 30 MPa, 35MPa and 40MPa is carried out. The simulation results are shown in Fig. 4. It revealed that an intense expansion cooling process occurred near the outfall. When hydrogen is vented into the atmosphere, the pressure rapidly reduces to ambient pressure, the released hydrogen expanded transiently and the pressure energy is converted into the kinetic energy. At the location  $L/D=7$  where the Mach disk is generated, the expansion ratio is very large, and the hydrogen temperature decreases to a valley value about 40 K. It can also be concluded that the locations of Mach disk formed under the three different filling pressures are basically the same, and the peak values of the Mach numbers are about 5.71.



(a) Axial velocity distribution

(b) Axial temperature distribution

Figure 4. Axial flow characteristics of hydrogen under different pressure

In the rear of mach disk, the current temperature rapidly increases to the ambient temperature 300K. Then, the jet flow kept on expanding, the hydrogen temperature decreased gradually while the flow velocity increases. The hydrogen velocity reaches a second peak at about  $L/D=38$ , and the flow temperature drops to about 211K. In this process, the flow velocity increasing rate and temperature decreasing rate are inversely proportional to the hydrogen filling pressures. After experiencing a

second expansion process, the momentum exchange between the leakage hydrogen and outer air is strengthened gradually, and the hydrogen velocity begins to decrease while the jet flow temperature increases slowly. The hydrogen velocity decay rate and temperature rising rate are inversely proportional to the filling pressures.

The propagation process of the hydrogen cloud generated by hydrogen release can be divided into two stages i.e. the radial expanding stage and the axial expanding stage. Fig. 5 shows the transferring and variation of the combustible cloud formed by hydrogen discharge during the prior 0.6s under 30 MPa filling pressure, in which the combustible region is determined according to the hydrogen flammable range of 4%-74% in air. When the high-pressure hydrogen is jetted into the open atmosphere, the discharged hydrogen expands strongly around the outlet due to the influence of the gas resistance. As shown in Fig. 5(a), the hydrogen cloud is apple-shaped and it expands slowly in the jet direction. After the Mach disk, the air begins to penetrate into the central core of the jet. After 0.3s, the axial diffusion rate increases gradually and the discharged hydrogen cloud grows to a big hydrogen balloon.

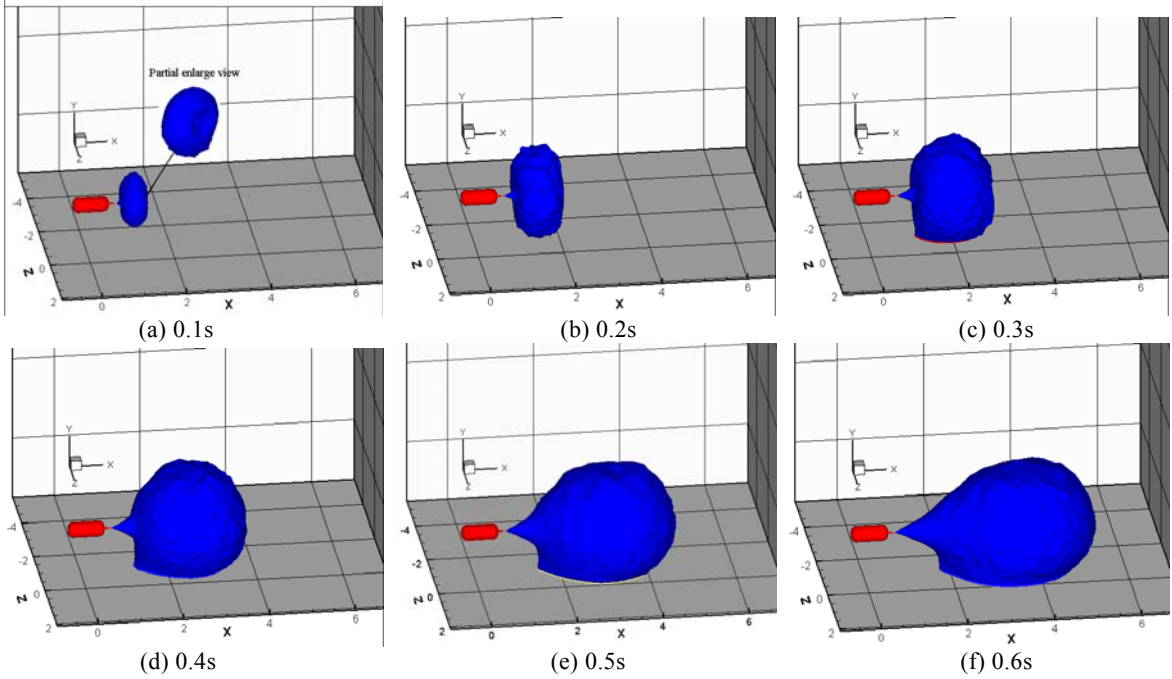


Figure 5. Flammable cloud propagation of hydrogen (4% molar isocontour)

**4.0 CONCLUSIONS**

In this paper, a 3-D mathematical model is established to study the high-pressure hydrogen discharge process. Results showed that a large expansion ratio jet is caused by the hydrogen discharge. The Mach disk is generated at  $L/D=7$  where the velocity and temperature of the hydrogen flow reach to the peak values, respectively. In addition, the variation of filling pressure has little influence on the peak values of the velocity and temperature of the flow during the considered pressure region. After the Mach disk, the variation rates of the hydrogen flow speed and temperature are in inversely proportional to the hydrogen filling pressures, the flow velocity and temperature reach second peak values at about  $L/D=38$ . At the initial period of the discharge, the

hydrogen cloud is apple-shaped, and the combustible cloud propagates along both the radial and axial directions with the passage of time.

## REFERENCES

1. Tzimas, E., Filiou, C., Peteves, S.D. and Veyret, J.B., Hydrogen Storage: State-of-the-art and Future Perspective, report of European Communities, 2003, Petten, European Commission.
2. Adamson, K.A., Pearson, P., Hydrogen and methanol: a comparison of safety, economics, efficiencies and emissions, *Journal of Power Sources*, **86**, No. 1-2, 2000, pp. 548-555.
3. Rosyid, O.A., Jablonsk, D. and Hauptmanns, U., Risk analysis for the infrastructure of a hydrogen economy, *International Journal of Hydrogen Energy*, **32**, No. 15 , 2007, pp. 3194-3200.
4. Liu, Y.L., Zheng, J.Y., Zhao, Y.Z., et al, Numerical simulation of barrier influence on diffusion of natural gas due to pipeline failure, *Journal of Petrochemical Universities*, **20**, No. 4, 2007, pp. 81-84.
5. Venetsanos, A.G., Baraldi, D., Adams, P., et al, CFD modeling of hydrogen release, dispersion and combustion for automotive scenarios, *Journal of loss prevention in the process industries*, **21**, No. 2, 2008, pp. 162-184.
6. Takano, K., Okabayashi, K., Kouchi, A., et al, Dispersion and explosion field tests for 40MPa pressurized hydrogen, *International Journal of Hydrogen Energy*, **32**, No. 13, 2007, pp. 2144-2153.
7. Shirvill, L.C., Roberts, P., Butler, C.J., et al, Characterization of the hazards from jet releases of hydrogen, 1st International Conference on Hydrogen Safety, 8-10 September 2005, Italy.
8. Olvera, A.H. and Choudhuri, A.R., Numerical simulation of hydrogen dispersion in the vicinity of a cubical building in stable stratified atmospheres, *International Journal of Hydrogen Energy*, **31**, No. 15, 2006, pp. 2356-2369.
9. Wilkening, H. and Baraldi, D., CFD modeling of accidental hydrogen release from pipelines, *International Journal of Hydrogen Energy*, **32**, No. 13, 2007, pp. 2206-2215.
10. Granovskiy, E.A., Lyfar, V.A., Skob, Y.A. and Ugryumov, M.L., Numerical modeling of hydrogen release, mixture and dispersion in atmosphere, 2nd International Conference on Hydrogen Safety, 11-13 September 2007, Spain.
11. Menter, F.R., Two-Equation Eddy-Viscosity Turbulence Models for Engineering Applications, *AIAA Journal*, **32**, No. 8, 1994, pp. 1598-1605.